JOURNAL OF GEOPHYSICAL RESEARCH, VOL. 98, NO. B12, PAGES 22,429–22,441, DECEMBER 10, 1993

Can Remanence Anisotropy Detect Paleomagnetic Inclination Shallowing Due to Compaction? A Case Study Using Cretaceous Deep-Sea Limestones

JOSEPH PAUL HODYCH AND SATRIA BIJAKSANA

Department of Earth Sciences, Memorial University of Newfoundland, St. John's, Newfoundland, Canada

We studied 35 Cretaceous limestone specimens from five Pacific plate Deep Sea Drilling Project sites. Inclination I_N of the natural remanence is on average 17° shallower than the average 44° expected paleofield inclination I. Anhysteretic remanence (ARM) applied identically to various axes was found to be weakest (ARM_{min}) perpendicular to bedding and strongest (ARM_{max}) parallel to bedding. The average ARM_{min}/ARM_{max} of 0.87 as well as the inclination shallowing of 17° likely originated from sediment compaction rotating the long axes of magnetite grains toward the bedding plane. This origin is theoretically and experimentally consistent with the average fractional compaction of 0.6 experienced by our sediments (estimated from their porosity). A compaction origin is also supported by the significant correlation found between tan I_N/tan I and ARM_{min}/ARM_{max}. The correlation line's slope of 2.3 ± 0.7 agrees with theory, taking into account our observation that ARM given perpendicular to the long axes of magnetite grains has on average ~0.37 times the intensity of ARM given axially. These results suggest that compaction-induced inclination shallowing may be detected in a suite of fine-grained magnetite-bearing sediments by looking for a correlation between tan I_N and ARM_{min}/ARM_{max} (having shown that ARM anisotropy is foliated in the bedding plane). This correlation line's prediction of I_N when $ARM_{min}/ARM_{max} = 1$ should estimate I corrected for inclination shallowing.

INTRODUCTION

Paleomagnetism can provide estimates of the paleolatitude at which rocks formed. The shallower the inclination I_N of natural remanence relative to bedding, the lower the paleolatitude L, as given by

$$L = \tan^{-1} \left(\tfrac{1}{2} \tan I_N \right). \qquad (1)$$

Equation (1) assumes that I_N is the same as the inclination I of the Earth's magnetic field when the rock formed. However, for sediments, I_N may be less than I for reasons reviewed by *Verosub* [1977]. For example, remanence acquired along the Earth's magnetic field at deposition may be deflected to shallower inclination when burial compacts the sediments. Such inclination shallowing will cause underestimation of paleolatitude.

The theory of compaction-induced inclination shallowing is discussed by *Blow and Hamilton* [1978], *Anson and Kodama* [1987], and *Arason and Levi* [1990*a*]. Such inclination shallowing has been observed in laboratory compaction of clay-rich sediments [e.g., *Blow and Hamilton*, 1978; *Anson and Kodama*, 1987; *Deamer and Kodama*, 1990]. It is accompanied by an increase in the anhysteretic remanence (ARM) anisotropy of the sediments [*Kodama and Sun*, 1990, 1992]; that is, to give the sediments an ARM becomes harder parallel to the compaction axis and easier at right angles.

Compaction and the inclination shallowing it induces are expected to be greatest in fine-grained sediments such as those deposited in the deep sea. Some soft deep-sea sediments do show inclination shallowing that is likely compaction-induced [e.g., *Celaya and Clement*, 1988; *Arason and Levi*, 1990*b*; *Collombat et al.*, 1990]. Recently, *Gordon* [1990] reported inclination shallowing in lithified deep-sea sedimentary rocks of Cretaceous age from many Deep Sea Drilling Project (DSDP) sites in the Pacific plate. *Tarduno* [1990] confirmed this inclination shallowing with more remanence measurements and strengthened the argument of *Gordon* [1990] favoring sediment compaction as the cause.

We set out to measure the ARM anisotropy of some of these rocks studied by *Gordon* [1990] and *Tarduno* [1990] to further test whether inclination shallowing was compaction-induced. If it was, the ARM anisotropy should be foliated in the bedding plane [*McCabe et al.*, 1985]. Also, we were searching [*Bijaksana and Hodych*, 1992] for a correlation between inclination shallowing and ARM anisotropy, since both were enhanced by compaction in the experiments of *Kodama and Sun* [1990]. We hoped that such a correlation would help us use ARM anisotropy to detect inclination shallowing in other sedimentary rocks. Indeed, *Jackson et al.* [1991] and *Collombat et al.* [1990] have suggested that ARM anisotropy can be used to detect and correct inclination shallowing. However, there are possible difficulties. For example, equidimensional magnetic grains may contribute to inclination shallowing (as discussed theoretically by Arason and Levi [1990a]) without contributing to ARM anisotropy.

DESCRIPTION OF SPECIMENS

Sampling

We measured 36 sedimentary rock specimens of Cretaceous age from five equatorial DSDP sites in the Pacific plate (Figure 1). Each of these sites shows inclination shallowing according to *Tarduno* [1990] (Table 1).

Our specimens were oriented cylinders of 19 mm diameter and 19 mm length which we drilled from the original 62 mm diameter DSDP cores. The horizontal plane was marked on each specimen assuming that the original DSDP

Paper number 93JB02022.
0148-0227/93/93JB-02022$05.00

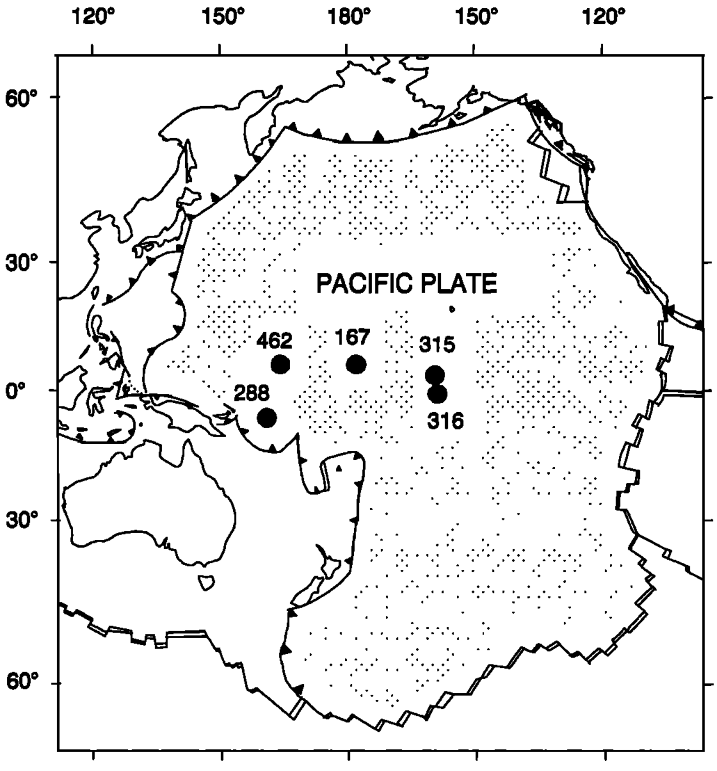

Fig. 1. The DSDP sites from which our specimens came.

drill holes were vertical. The true azimuth of our specimens, like that of the original DSDP cores, was unknown. Each specimen is assigned a number such as 167-62-4-64 (Table 2), which indicates that the specimen is from DSDP site 167, core 62, section 4 at a depth of 64 cm in that section.

Composition

Our specimens are all very fine-grained and light in color (white to gray). No sedimentary structures were visible except in 14 specimens (indicated by an asterisk in Table 2) which appear to be bioturbated (they are mottled probably because of burrows deformed by compaction). The specimens are all well lithified but porous.

X ray diffraction was used to identify the minerals in each specimen and to semiquantitatively estimate their relative proportions. For a small powdered sample of each specimen, intensity of diffracted radiation was plotted against 2θ (twice the diffraction angle) as 2θ was varied from 3° to 60°. A Rigaku RU200 diffractometer with a copper X ray tube was used. The only minerals detected in large amounts were calcite and quartz. (Significant clay minerals were detected only in specimens 462-55-3-29 and 462-55-3-132.) The proportion of calcite in each specimen was estimated from the area under the 29.7° 2θ calcite peak multiplied by 1.65, and the proportion of quartz was estimated from the area under the 26.7° 2θ quartz peak. (Areas were approximated by multiplying peak height by width at half height.) The semiquantitative estimates of calcite content are listed in Table 2. Almost all specimens can be termed limestones (more than half calcite according to *Reijers and Hsü* [1986]). Only specimen 315A-26-2-123 can confidently be termed a claystone (dominated by siliciclastic grains, more than two thirds of which are <4 μm in diameter according to *Stow and Piper* [1984]). Earlier, we had assumed [*Bijaksana*, 1991; *Bijaksana and Hodych*, 1992) that our

TABLE 1. Paleomagnetic Data Averaged by Site

DSDP Site	Stage	Mean Age, Ma	D, deg	I, deg	N	$\bar{I}_N$, deg	I_{95}, deg	$\Delta\bar{I}$, deg This Study	$\Delta\bar{I}'$, deg *Tarduno* [1990]
167	Albian to Hauterivian	116	23.3	-38.0	7	-26.7	±8.8	13.6	8.7
288A	Turonian to Albian	92	5.5	-56.7	8	-47.5	±16.0	9.2	14.7
315A	Campanian to Santonian	79	13.5	-42.2	8	-13.8	±7.2	28.4	20.2
316	Maastrichtian to Campanian	73	9.6	-41.8	6	-23.0	±14.2	18.8	20.9
462	Campanian	79	-7.2	-39.8	5	-14.5	±6.9	25.3	32.1

Mean age is estimated from *Harland et al.* [1990]. D and I are the declination and inclination, respectively, of the paleofield at the site, estimated from the APWP for the Pacific plate. N is the number of specimens we studied at the site. $\bar{I}_N$ is the site average inclination of natural remanence, and I_{95} is its 95% confidence interval [*McFadden and Reid*, 1982]. $\Delta\bar{I}$ is the average inclination shallowing that we observe at the site, and $\Delta\bar{I}'$ is that observed by *Tarduno* [1990].

TABLE 2 Specimen Properties

						ARM and Its Anisotropy					
Specimen	Calcite Content, %	ρ, g cm^{-3}	Φ	ΔV	ΔI, deg	h_A, %	H_{MD}, mT	ARM_{max}, A/m	ARM_{int}/ARM_{max}	ARM_{min}/ARM_{max}	$\bar{K}$, $\times 10^{-3}$ SI
167-62-4-64	49	1.63	0.39	0.54	5.9	6.2	22	1.01	0.993	0.938	0.33
167-63-4-75*	95	2.0	-----	-----	20.1	12.0	14	1.13	0.983	0.883	0.47
167-65-3-42	91	2.08	0.21	0.64	-1.2	12.9	25	1.23	0.991	0.872	0.37
167-67-3-36*	83	2.12	0.21	0.65	7.4	11.2	18	0.52	0.986	0.890	0.14
167-69-4-133	92	2.15	0.23	0.64	-----	2.6	20	0.45	0.994	0.974	0.10
167-71-2-63*	95	2.16	0.19	0.65	17.0	18.8	26	1.29	0.995	0.813	0.26
167-72-2-63*	98	2.2	-----	-----	10.9	7.8	23	0.38	0.985	0.923	0.09
167-73-2-121	97	2.23	0.17	0.66	18.9	3.2	22	0.07	0.990	0.968	0.04
288A-21-2-98	93	1.96	0.28	0.61	0.5	7.1	18	0.41	0.993	0.929	0.13
288A-21-3-18	91	1.86	0.30	0.60	2.5	8.3	23	0.51	0.991	0.917	0.17
288A-22-2-82	86	1.98	0.27	0.62	6.7	13.2	27	0.84	0.990	0.869	0.30
288A-23-1-79	67	1.97	0.25	0.63	-1.4	1.0	20	0.12	0.990	0.990	0.03
288A-23-2-115	90	1.94	0.27	0.62	45.3	11.2	19	0.41	0.966	0.892	0.11
288A-23-3-76	73	1.87	0.31	0.60	4.0	8.2	22	0.60	0.998	0.917	0.19
288A-26-1-28	74	1.79	0.38	0.55	8.2	10.5	33	0.41	0.970	0.898	0.44
288A-29-1-47	59	2.17	0.19	0.66	9.0	8.5	23	0.48	0.988	0.916	0.26
315A-19-5-50*	96	2.08	0.31	0.60	30.3	18.3	20	0.93	0.990	0.818	0.87
315A-20-2-21*	93	2.38	0.13	0.68	26.6	16.9	18	1.54	0.998	0.832	1.74
315A-20-2-131*	97	2.19	0.18	0.66	27.3	16.1	18	1.32	0.989	0.841	2.25
315A-20-5-17*	99	1.92	0.31	0.59	32.3	12.8	18	0.46	0.991	0.873	0.56
315A-21-2-11*	99	2.13	0.21	0.65	38.7	26.1	35	0.79	0.997	0.740	1.02
315A-21-5-8*	94	2.12	0.22	0.64	27.3	18.4	28	0.49	0.990	0.818	0.48
315A-21-6-108*	87	1.93	0.28	0.61	13.5	11.3	28	0.16	0.982	0.889	0.32
315A-26-2-123	37	1.98	0.21	0.64	30.8	15.7	37	0.48	0.992	0.845	0.59
316-19-2-108	98	2.26	0.20	0.65	13.3	19.4	34	0.69	0.984	0.809	0.32
316-19-4-74	98	2.22	0.23	0.64	-----	24.5	30	0.33	0.986	0.758	0.33
316-20-4-67*	98	2.01	0.32	0.59	25.6	8.5	25	0.37	0.996	0.915	0.14
316-22-2-77	98	2.3	-----	-----	31.8	19.1	27	0.35	0.988	0.812	0.30
316-23-3-107	99	2.23	0.26	0.62	22.7	27.3	25	0.77	0.974	0.735	1.27
316-24-3-59*	94	2.2	-----	-----	0.5	17.7	27	0.49	0.994	0.824	0.33
316-25-5-40*	97	2.06	0.29	0.61	18.6	18.7	30	0.62	0.997	0.813	0.36
462-55-1-28	100	1.6	0.37	0.55	25.5	9.8	23	0.41	0.985	0.903	0.77
462-55-1-114	99	1.6	-----	-----	17.8	7.6	22	0.11	0.993	0.925	0.15
462-55-2-128	98	1.6	-----	-----	27.3	6.6	27	0.45	0.989	0.935	0.38
462-55-3-29	60	1.8	-----	-----	29.2	21.5	26	2.10	0.983	0.789	-----
462-55-3-132	54	1.9	-----	-----	26.8	19.6	20	1.37	0.989	0.806	-----

* Samples that appear bioturbated. Estimates of calcite content are semi-quantitative. ρ is density. Φ is porosity. ΔV is compaction. ΔI is inclination shallowing. h_A is percentage ARM anisotropy. H_{MD} is median destructive field for ARM. ARM_{max}, ARM_{int}, and ARM_{min} are the intensities of the maximum, intermediate, and minimum principal ARM respectively, normalized to 0.1 mT biasing field. $\bar{K}$ is mean volume magnetic susceptibility in SI units [*Shive*, 1986].

Fig. 2. Deep-sea limestone specimen 315A-21-2-11 viewed with a scanning electron microscope on a surface broken perpendicular to bedding. The dotted line indicating 6 μm is parallel to bedding.

specimens from sites 315A and 462 were claystones, because of their designation in the orginal DSDP graphic lithology logs.

Eight of the specimens (at least one per site) were viewed at right angles to bedding, using a scanning electron microscope with semiquantitative analysis capability. The calcite was commonly found to be in grains a few microns across. Some of these grains were obviously coccolith fragments, and presumably most if not all of the calcite is of biogenic origin. Quartz was in angular grains, presumably of terrestrial origin. No iron oxide grains were identified. No overall preferred orientation of calcite grains was noticeable even in a sample like 315A-21-2-11 with high ARM anisotropy (Figure 2).

Porosity, Density and Compaction

The fractional porosity Φ was measured for most specimens (Table 2) using a pycnometer (Beckman model 930). This forced air at 2 atm pressure into the pores of the air-dried specimens.

The density ρ of each air-dried specimen was also measured (from mass and volume) to check the reliability of the porosity measurements. The density of a dry rock with grains of density ρ_s should be given [*Hamilton*, 1976] by

$$\rho = (1 - \Phi)\,\rho_s. \qquad (2)$$

Hence, plotting ρ versus Φ should give a line with a slope of $-\rho_s$ and with a ρ intercept of ρ_s. Our limestone specimens do show a correlation between ρ and Φ (Figure 3) that is significant with 99.9% confidence (R=0.872, N=28). The correlation line has a slope of -2.4±0.3 and a ρ intercept of 2.7±0.1, in agreement with ρ_s = 2.7 g/cm³ expected for calcite grains.

The porosity determinations should be accurate enough to estimate the approximate degree of compaction undergone by the limestones since deposition. Compaction (fractional volume change) ΔV should be given [*Arason and Levi*, 1990*b*] by

$$\Delta V = \frac{\Phi_o - \Phi}{1 - \Phi}, \qquad (3)$$

where Φ_o is the initial porosity, assuming no migration of calcite in or out of the specimen. From observations of porosity of deep-sea calcareous sediment on the present seafloor [*Hamilton*, 1976], we expect Φ_o to have been approximately 0.72±0.06. With this assumption, (3) yields estimates of ΔV for our specimens (Table 2) ranging from 0.54±0.10 to 0.68±0.07 with an average ΔV of 0.62±0.10.

ESTIMATION OF INCLINATION SHALLOWING

The natural remanence of each specimen was measured using a superconducting magnetometer (CTF Systems Inc., Port Coquitlam, British Columbia). Change in remanence was monitored during stepwise alternating field (AF) demagnetization applied with a Schonstedt model GDS-1 demagnetizer. Demagnetization steps of 2.5 mT were used up to 20 mT; these were followed by steps of 5 mT up to 40 mT and then by steps of 10 mT. Demagnetization was continued until remanence fell to less than 10% of its original intensity. This usually required peak fields of 60 mT but occasionally required up to 90 mT. The ability of 90 mT or less to demagnetize the remanence suggests that it is carried by magnetite rather than hematite.

Remanence directions often changed during demagnetization to 15 mT but ceased changing significantly in the 20 mT and higher demagnetization steps (except for specimens 167-69-4-133 and 316-19-4-74, whose remanence directions never ceased changing). The inclination I_N and declination of this higher-coercivity (>20 mT) remanence component

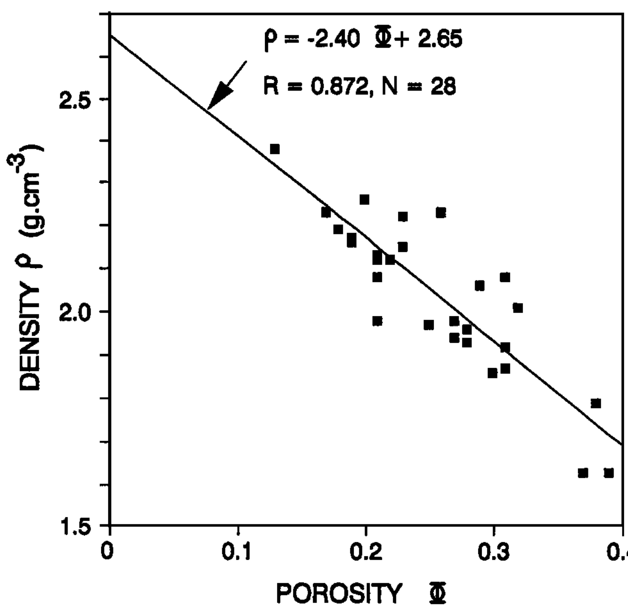

Fig. 3. Correlation between density ρ and porosity Φ of our air-dried limestone specimens.

were determined using least squares fitting on vector plots (following *Kirschvink* [1980]). Typical behavior upon demagnetization is shown by the vector plots of Figure 4.

The paleoinclination I of the Earth's field at each site (Table 1) was predicted from the Pacific plate's apparent polar wander path (APWP) by linearly interpolating between the reference poles of 66 Ma and 81 Ma from *Gordon* [1983], 94 Ma from *Sager and Pringle* [1988], and 125 Ma from *Gordon* [1990]. (Average I is 44°.) Following *Arason and Levi* [1990*a*], inclination shallowing ΔI is taken as the difference between I and I_N, with inclination changes towards lower absolute values taken as positive inclination shallowing.

Table 2 lists ΔI for each specimen. Note that ΔI estimates for individual specimens may be in error by ±14° owing to incomplete averaging out of paleosecular variation [*Irving and Pullaiah*, 1976]. The specimens likely carry a post-depositional detrital remanence (pDRM), as will be discussed later. Deep-sea sediments accumulating at 1 cm or more per 10^3 years are estimated to acquire pDRM at a burial depth of about 16 cm [*deMenocal et al.*, 1990]. Accumulation rates of a little over 1 cm per 10^3 years seem typical of deep-sea calcareous sediments (judging from the observations of *Tauxe and Wu* [1990]). Hence, our limestone specimens likely magnetized over a period of less than 10^4 years, which is less than the 10^5 years that may be needed to average out secular variation [*Butler*, 1992, p. 163].

As can be seen in Table 1, our mean ΔI for each site agrees (within its 95% confidence interval) with that of *Tarduno* [1990], which was based on many more specimens. This shows that our specimens, although few in number, have inclination errors that are reasonably representative of their sites.

MEASUREMENT OF MAGNETIC ANISOTROPY

ARM Anisotropy of the Limestones

Our procedure in ARM anisotropy measurements was similar to that of *McCabe et al.* [1985]. After AF demagnetizing in at least 70 mT, the specimen was given an ARM by coaxially applying a constant biasing field of 0.2 mT and an alternating field of 70 mT peak strength, which was slowly reduced to zero. The resulting ARM intensity was measured and averaged with an ARM given in the same way in the opposite direction. This was repeated for the nine axes recommended by *Girdler* [1961].

Stephenson and Potter [1989] warned that gyromagnetic remanence may be produced along with ARM in anisotropic rocks with magnetite grains in the 0.1 to 10 μm size range. Such grains are probably common in our specimens. However, because our specimens have little anisotropy in the bedding plane, gyromagnetic remanence should be produced perpendicular to the AF axis and should not affect our ARM measurements, since they are always made parallel to the AF axis. We tested this for two of our most anisotropic specimens (315A-21-5-8 and 316-23-3-107). We applied 70 mT AF to an axis in the specimen (after tumble demagnetization in 80mT AF) and then measured the magnetization along that axis. This was repeated for the nine axes used in ARM anisotropy determination. Any gyromagnetic remanence produced was always less than 0.6% of the ARM in the anisotropy determination and could be neglected.

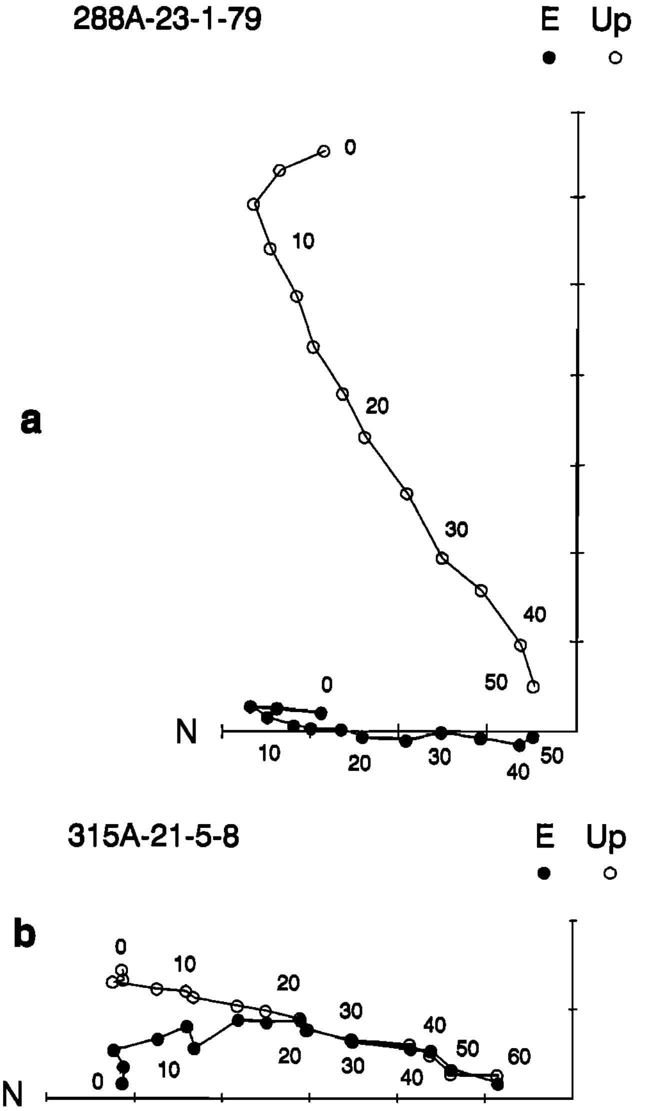

Fig. 4. Typical behavior of the natural remanence of our limestone specimens during demagnetization by alternating fields, whose intensity is given in milliteslas. Symbols indicate the projection of magnetization vectors onto the horizontal plane (solid circles) and onto the north-south vertical plane (open circles). Scale divisions represent 5×10^{-4} A m^{-1} for the Figure 4*a* and 5×10^{-3} A m^{-1} for Figure 4*b*.

Following *McCabe et al.* [1985], ARM anisotropy was treated as a second-rank tensor (like susceptibility anisotropy). The ARM data were used to determine the least squares fit anisotropy tensor [*Girdler*, 1961]. The ARM magnitudes predicted by this tensor were always very close to the ARM magnitudes observed [*Bijaksana*, 1991], indicating that the ARM anisotropy is well described by a triaxial ellipsoid [*McCabe et al.*, 1985]. The magnitudes and directions of the three principal axes of the anisotropy ellipsoid were calculated. (Their azimuthal orientation was approximated assuming that the declination of high coercivity natural remanence equals D in Table 1.) Table 2 lists the results, including the percent ARM anisotropy h_A, which is defined following *McCabe et al.* [1985] and *Kodama and Sun* [1990] as

$$h_A = 100\,(\mathrm{ARM}_{max} - \mathrm{ARM}_{min})/\mathrm{ARM}_{int}, \tag{4}$$

where ARM_{max}, ARM_{int}, and ARM_{min} are ARM magnitudes along the maximum, intermediate, and minimum principal axes, respectively. (Our ARM magnitudes were divided by 2 to normalize them to the 0.1 mT biasing field used by *McCabe et al.*, [1985].)

Figure 5 presents equal area stereographic plots of the directions of ARM_{max} and ARM_{min} axes for specimens at each site (following the convention of *Ellwood et al.* [1988]). The ARM_{min} axis is oriented on average at $6° \pm 5°$ to vertical, that is, almost perpendicular to bedding (excluding specimen 288A-23-1-79, whose anisotropy is too low for orientation to be accurately measured, and specimen 288A-23-2-15 which is clearly anomalous). Average h_A is $13\% \pm 7\%$. Anisotropy within the bedding plane is low, as shown by magnetic lineation ARM_{max}/ARM_{int}, averaging 1.01 ± 0.01. ARM anisotropy is strongly foliated in the bedding plane, with magnetic foliation ARM_{int}/ARM_{min} averaging 1.15 ± 0.09.

ARM Anisotropy of Magnetic Particles in the Limestones

The average ARM anisotropy of individual magnetic particles in an assemblage can be estimated using a sample prepared by mixing the particles in a glue and aligning their long axes with a strong magnetic field while the glue hardens. This was done with magnetite particles in epoxy by *Jackson et al.* [1991]. We applied a similar method to five of our limestone specimens.

About 3 g of a limestone specimen was crushed and placed in a buffered (pH 4) acetic acid solution to dissolve the calcite. This dissolution method follows DSDP standard procedures that leave iron oxides unaltered [*Freeman*, 1986]. After calcite dissolution was complete, the remaining particles were washed and mixed with warm liquid gelatin which was allowed to set in a small plastic cup, producing a solid sample of about 12 cm^3 volume. The sample was given an anhysteretic remanence (as in the preceding section), and its AF demagnetization curve was found to be

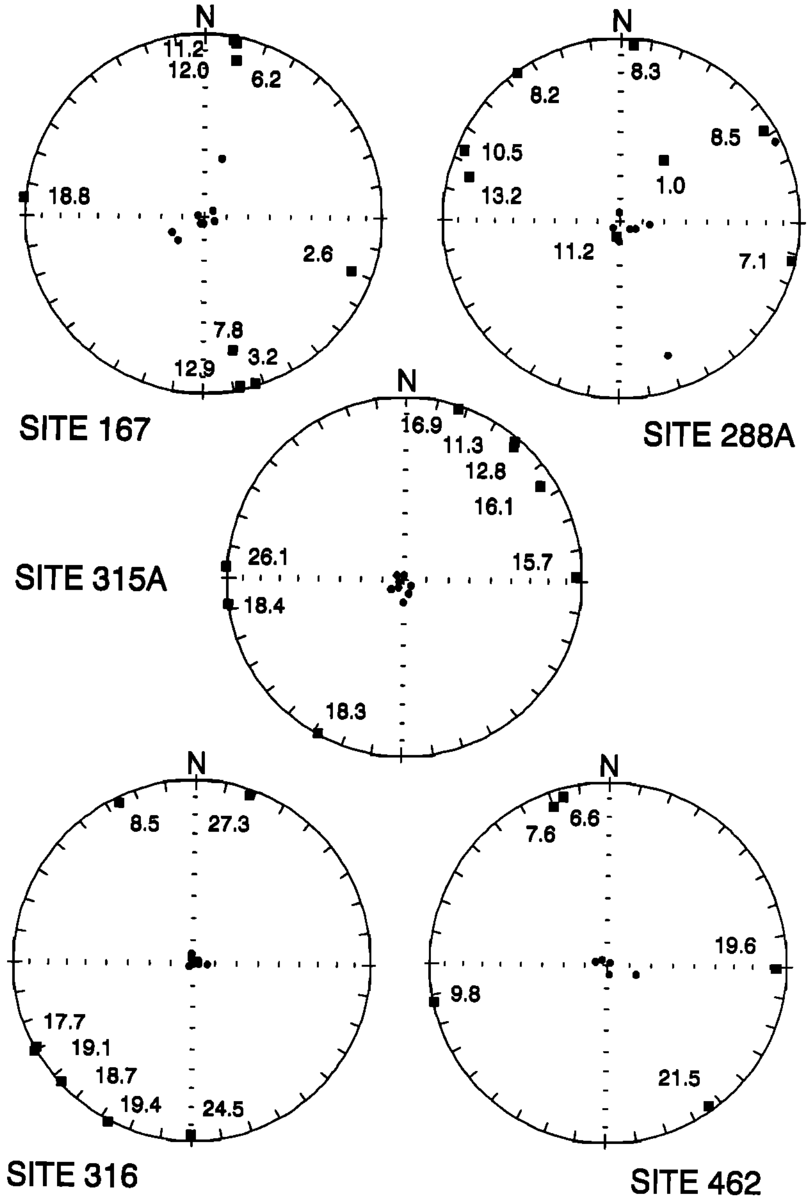

Fig. 5. The directions of ARM_{max} and ARM_{min} axes are shown by large solid squares and small solid circles, respectively, on the lower hemispheres of equal area plots (bedding is assumed to be horizontal). Next to each large solid square is the magnitude of h_A, the percent ARM anisotropy.

almost identical to that of the anhysteretic remanence of the original limestone. The same was found for the other samples, showing that dissolution probably did not alter the magnetic grains and that the gelatin does harden enough to immobilize the magnetic grains.

Each sample was then warmed to liquify the gelatin, stirred, and placed in a horizontal 90 mT aligning field while the gelatin cooled and hardened. The sample was demagnetized and given an anhysteretic remanence (as above) along the grain alignment direction. This anhysteretic remanence magnitude (normalized to 0.1 mT biasing field) is designated $ARM_{\parallel}$. Similarly, anhysteretic remanences were given in a vertical and in a horizontal direction perpendicular to the alignment direction; these two anhysteretic remanences had similar intensities and were averaged, normalized, and designated $ARM_{\perp}$. For each sample, we repeated this procedure after taking half of the sample and diluting it with an equal volume of gelatin and usually found that $ARM_{\perp}/ARM_{\parallel}$ decreased. For some samples, this procedure had to be repeated another three or four times before $ARM_{\perp}/ARM_{\parallel}$ stopped decreasing with dilution (Figure 6). Presumably, at insufficient dilution, neighboring particles inhibit the magnetic grains from completely aligning with the 90 mT field. The average $ARM_{\perp}/ARM_{\parallel}$ that is stable to further dilution is used (Table 3) as an estimate of the ratio of ARM perpendicular and parallel to the long axes of the magnetic particles.

Susceptibility Anisotropy

For each of our specimens, magnetic susceptibility was measured along six orientations (two measurements for each orientation) using a Bartington model MS2 susceptibility meter. Average volume susceptibility $\overline{K}$ is listed in Table 2. A computer program (AMS-BAR, Morris Magnetics Inc.) was then used to calculate the magnitudes and directions of the three principal susceptibilities. Many specimens had a $\overline{K}$ too weak for anisotropy to be reliably determined; we rejected specimens with significantly more than 1% rms error (defined as the root-mean-square of the differences between repeat measurements of the same matrix element divided by $\overline{K}$). Results for the remaining 20 specimens are given in Table 4, with percent susceptibility anisotropy h_K defined [*Howell et al.*, 1958] as

$$h_K = 100\ (K_1 - K_3)/K_2, \qquad (5)$$

where K_1, K_2, and K_3 are the maximum, intermediate, and minimum principal susceptibilities [*Ellwood et al.*, 1988].

Susceptibility anisotropy was measured after ARM anisotropy and hence may be affected by field-impressed susceptibility anisotropy [*Potter and Stephenson*, 1990]. Any such effect was evidently not great enough to change the basic shape of the susceptibility ellipsoid, which is strongly foliated in the bedding plane like the ARM ellipsoid.

DISCUSSION

Origin of the Natural Remanence

The natural remanence is probably carried by magnetite rather than hematite in all of our specimens. This follows from the ability of 90 mT or less to AF demagnetize the remanence. It is also consistent with the absence of red coloration and with the evidence of natural remanence carried by magnetite in all 10 specimens from site 462 that were thermally demagnetized by *Steiner* [1981].

The magnetite grains are probably a few microns or less in diameter, judging by the typical sizes of other mineral grains seen with the scanning electron microscope. We would expect magnetite of this grain size to be pseudo-single-domain or single-domain [*Dunlop*, 1981]. For most specimens, natural remanence of coercivity between 20 mT and 60 mT was used to determine inclination. This range of coercivity is consistent with pseudo-single-domain or single-

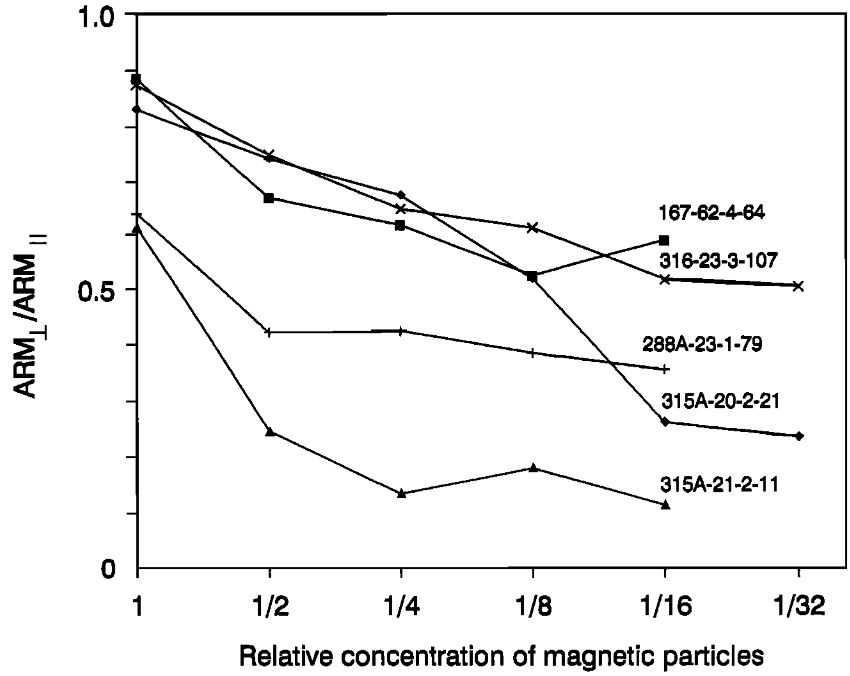

Fig. 6. Magnetic particles extracted from five of our limestone specimens were dispersed in gelatin and had their long axes aligned by a 90 mT field. The ratio of ARM given perpendicular and parallel to the aligning axis is plotted as a function of the relative concentration of the magnetic particles in the gelatin matrix.

TABLE 3. Magnetic Particle Anisotropy Determinations Used To Predict Specimen Anisotropy

Specimen	ΔV	$ARM_{\perp}/ARM_{\parallel}$	ARM_{min}/ARM_{max} Predicted from (10) (b=0.63)	ARM_{min}/ARM_{max} Predicted from (13) (b=0.63)	ARM_{min}/ARM_{max} Observed
167-62-4-64	0.54	0.56	0.66	0.92	0.94
288A-23-1-79	0.63	0.37	0.60	0.84	0.99
315A-20-2-21	0.68	0.25	0.57	0.77	0.83
315A-21-2-11	0.65	0.15	0.59	0.72	0.74
316-23-3-107	0.62	0.51	0.61	0.89	0.74

Here ΔV is fractional compaction, $ARM_{\perp}/ARM_{\parallel}$ is the magnetic particle anisotropy parameter, and ARM_{min}/ARM_{max} is the specimen anisotropy parameter.

domain magnetite [*Dunlop*, 1981]. The former is favored by all five of our determinations of $ARM_{\perp}/ARM_{\parallel}$ being significantly greater than zero.

King et al. [1983] have suggested that the ratio of ARM intensity (normalized to 0.1 mT biasing field) to magnetic susceptibility can be used to identify samples with similar magnetite grain sizes in sedimentary sequences. This ratio for our specimens is on average 2.1×10^3, similar to that found by *Tauxe and Wu* [1990] for magnetite-bearing deep-sea carbonate sediments whose ratio of saturation remanence to saturation magnetization ranges from 0.16 to 0.22, suggesting pseudo-single-domain grains.

The theoretical and experimental study of *Stephenson et al.* [1986] suggests that a plot of normalized principal susceptibilities ($K_1/(K_1+K_2+K_3)$, $K_2/(K_1+K_2+K_3)$, $K_3/(K_1+K_2+K_3)$) versus the corresponding normalized principal remanences should yield a straight line. The line's intercept p_o on the normalized susceptibility axis should lie between about 0.12 and 0.20 for multidomain grains and at 0.5 for elongated single-domain grains. We have estimated p_o for our specimens (Table 4) using ARM in place of the thermal or isothermal remanence used by *Stephenson et al.* [1986]. The mean p_o is 0.21 ± 0.06, suggesting that pseudo-single domain grains and multidomain grains are present.

The various estimators of domain state discussed here all suggest the presence of pseudo-single-domain magnetite, which is probably the dominant carrier of natural remanence in our specimens. We expect that the natural remanence is a pDRM because of the inferred fine grain size of the magnetite [*Verosub*, 1977] and because of the expectation that most of our specimens were bioturbated. (Fourteen specimens have a mottled, burrowed appearance. None of our specimens show the fine lamination that would prove absence of bioturbation.)

Origin of Inclination Shallowing

Gordon [1990] and *Tarduno* [1990] both favored compaction as the main cause of inclination shallowing in the

TABLE 4. Anisotropy of Magnetic Susceptibility

Specimen	h_A, %	h_K, %	K_1, $\times10^{-3}$ (SI)	K_2/K_1	K_3/K_1	Dec_1, deg	Inc_1, deg	Dec_3, deg	Inc_3, deg	p_o
167-62-4-64	6.2	4.9	0.34	0.978	0.952	280	9	10	1	0.12
167-63-4-75	12.0	3.2	0.48	0.973	0.969	109	14	219	53	0.27
167-65-3-42	12.9	4.3	0.38	0.978	0.958	25	20	198	70	0.25
288A-26-1-28	10.5	2.9	0.44	0.989	0.971	92	20	225	62	0.24
315A-19-5-50	18.3	10.4	0.90	0.980	0.898	335	1	71	83	0.16
315A-20-2-21	16.9	6.8	1.78	0.994	0.932	200	1	78	87	0.21
315A-20-2-131	16.1	6.5	2.30	0.994	0.935	181	0	86	87	0.20
315A-20-5-17	12.8	7.0	0.57	0.995	0.930	323	6	102	82	0.15
315A-21-2-11	26.1	5.9	1.04	0.992	0.941	126	4	258	85	0.27
315A-21-5-8	18.4	7.7	0.50	0.994	0.923	230	1	351	88	0.20
315A-21-6-108	11.3	7.8	0.33	0.984	0.923	193	2	57	87	0.11
315A-26-2-123	15.7	4.9	0.61	0.983	0.952	16	3	146	86	0.25
316-19-2-108	19.4	7.2	0.33	0.986	0.929	339	9	114	77	0.11
316-19-4-74	24.5	4.2	0.33	0.985	0.959	128	10	273	78	0.29
316-22-2-77	19.1	7.7	0.31	0.957	0.926	322	9	114	80	0.24
316-23-3-107	27.3	7.8	1.31	0.990	0.923	161	0	41	89	0.25
316-24-3-59	17.7	5.8	0.33	0.976	0.943	145	5	251	72	0.25
316-25-5-40	18.7	5.0	0.37	0.988	0.951	201	15	360	74	0.26
462-55-1-28	9.8	4.5	0.78	0.997	0.955	180	0	47	90	0.18
462-55-2-128	6.6	4.2	0.38	0.991	0.959	268	0	116	90	0.13

Here h_A is the percent ARM anisotropy, h_K is the percent magnetic susceptibility anisotropy, K_1, K_2, and K_3 are the maximum, intermediate, and minimum principal magnetic susceptibilities, respectively. (Mean susceptibility K is given in Table 2.) Dec_1 and Inc_1 (Dec_3 and Inc_3) are the declination and inclination of the maximum (minimum) susceptibility axis, and p_o is a parameter relating remanence anisotropy and susceptibility anisotropy [*Stephenson et al.*, 1986].

rocks we have studied. Other possible causes of inclination shallowing that they considered are the following. Viscous remanence could cause inclination shallowing but should have been removed from our specimens and those of *Tarduno* [1990] by the AF demagnetization. Even if present, viscous remanence could not explain why inclination shallowing is observed in reversely as well as normally polarized sediments [*Gordon*, 1990]. Similarly, drill stem remanence as a cause of inclination shallowing is ruled out by a positive reversal test [*Tarduno*, 1990]. Delay in remanence acquisition coupled with the Pacific plate's northward drift could cause inclination shallowing [*Gordon*, 1990]. However, the observed inclination shallowing would require tens of millions of years delay (estimating drift rate from work by *Zonenshain et al.* [1987]), whereas tens of thousands of years delay seems more typical of pDRM in deep-sea sediments [*deMenocal et al.*, 1990]. Too large a portion of the Pacific plate shows inclination shallowing for the shallowing to be due to motion of this portion of the plate relative to the whole [*Tarduno*, 1990]. Inaccuracies in the APWP causing inclination shallowing would not explain the paleolatitude dependence of the shallowing [*Tarduno*, 1990].

Tarduno [1990] showed that inclination shallowing is greatest for those of his sites magnetized at intermediate paleolatitudes, as is expected on the basis of the following theories for compaction-induced inclination shallowing. (For easy comparison, we have changed some symbols in the quoted references.) *Blow and Hamilton* [1978] assumed that remanence would behave like a passive line marker upon compaction and theoretically derived the equation

$$\tan (I - \Delta I) = (1 - \Delta V) \tan I, \qquad (6)$$

where remanence inclination is equal to I before and I-ΔI after compaction. *Anson and Kodama* [1987] showed that the modified equation

$$\tan (I - \Delta I) = (1 - b\Delta V) \tan I \qquad (7)$$

described inclination shallowing produced in their compaction experiments on synthetic sediments if $b=0.54\pm0.18$ for their equidimensional (0.5 μm diameter) magnetite grains and if $b=0.63\pm0.18$ for their acicular (0.45 μm by 0.075 μm) magnetite grains. Whereas Blow and Hamilton's theory is macroscopic in approach and Anson and Kodama's modification is empirical, *Arason and Levi* [1990*a*] showed that (7) can be derived theoretically using a variety of microscopic models in which compaction rotates magnetic grains in sediment. The value of b in (7) depends upon the microscopic model used; $b=1$ for magnetic needles that are initially perfectly aligned along the Earth's field in a soft matrix but should be lowered by grains being less elongated and more dispersed in alignment. Our average observed ΔI of $17.4° \pm 2.0°$ (standard error) and ΔV of 0.62 ± 0.10 are consistent with (7) when $b=0.8\pm0.2$. Our observations are also consistent with those of *Arason and Levi* [1990*b*], whose magnetite-bearing deep-sea clays obey (7) when $b=1$ to 2.

Comparison of ARM Anisotropy and Susceptibility Anisotropy

ARM anisotropy should be better suited than susceptibility anisotropy for detecting or correcting inclination shallowing in our specimens. One reason is that ARM and natural remanence are carried by magnetite grains with similar coercivity spectra in all of our specimens. Mean destructive field H_{MD} for ARM (Table 2) lies within the range of coercivity used to estimate ΔI. In contrast, magnetic susceptibility is probably due preferentially to those magnetite grains of lowest coercivity. A second reason is that ARM in any single-domain magnetite grains present will not show the inverse anisotropy displayed by susceptibility in such grains [*Rochette*, 1988; *Stephenson and Potter*, 1989]. A third reason is that in the experiments of *Kodama and Sun* [1990], h_A increased steadily as compaction progressed, whereas h_K either increased more erratically (when measured before h_A) or showed little increase (when measured after h_A). Finally, 40% of our specimens had too low a susceptibility for us to measure h_K accurately with a Bartington MS2 susceptibility meter.

Because susceptibility anisotropy can be measured quickly [*Rochette et al.*, 1992], one might hope to use it in place of ARM anisotropy, but theory suggests that this cannot be done accurately. From the theory of *Stephenson et al.* [1986] used earlier, it is easy to show that

$$h_K/h_A \approx 1 - 3p_o. \qquad (8)$$

Hence we do not expect to accurately predict h_A from h_K, since this requires estimating p_o, which depends on the size and domain state of the magnetic grains and varies from 0.11 to 0.29 in our specimens (Table 4).

Origin of the ARM Anisotropy

The ARM anisotropy of our specimens is strongly foliated in the horizontal bedding plane ($ARM_{int}/ARM_{min}=1.15$ on average), but is only weakly lineated ($ARM_{max}/ARM_{int}=1.01$ on average). This strong dominance of foliation over lineation implies that equidimensional magnetite grains are not contributing significantly to the ARM anisotropy of our specimens. Such grains have easy axes due to magnetocrystalline or stress-induced anisotropy [*Hodych*, 1990]. Only the Earth's magnetic field could align these easy axes, but it would produce an ARM anisotropy with lineation along the remanence direction rather than foliation in the bedding plane.

The ARM anisotropy in our specimens must be mainly due to magnetite grains with shape anisotropy, that is, to grains easiest to magnetize along their longest axes (where self-demagnetizing fields are weakest). Any preferred orientation of the longest axes acquired during deposition on the sea floor was probably erased by bioturbation. Hence we expect that most of the ARM anisotropy in our specimens was induced after deposition by sediment compaction that rotated magnetite grains so that their longest axes lie preferentially in the bedding plane [*Ellwood*, 1984]. Similar ARM foliation was produced perpendicular to compaction in the experiments of *Kodama and Sun* [1990] using clay containing synthetic acicular (0.45 μm by 0.075 μm) magnetite grains.

No mathematical theory has been explicitly derived for how the magnitude of ARM anisotropy increases with fractional compaction ΔV. However, *Arason and Levi* [1990*a*] have shown theoretically that inclination shallowing should increase with ΔV as in (7), assuming single-domain magnetite needles in a soft matrix. Also, *Jackson et al.* [1991] have shown theoretically that inclination shallowing should increase along with ARM anisotropy for detrital remanence in single-domain grains with shape anisotropy. Their equation (rewritten) is

$$\tan I_N = (\mathrm{ARM_{min}/ARM_{max}}) \tan I, \quad (9)$$

where $\mathrm{ARM_{max}}$ and $\mathrm{ARM_{min}}$ are (in effect) assumed to be parallel and perpendicular to the bedding plane respectively. Since $I_N = I\text{-}\Delta I$, it is easily seen that (9) has the form of (7), but with ($1\text{-}b\Delta V$) replaced by $\mathrm{ARM_{min}/ARM_{max}}$. Hence for both (9) and (7) to be true for single-domain magnetite needles in a soft matrix, we must have

$$\mathrm{ARM_{min}/ARM_{max}} = 1 - b\Delta V. \quad (10)$$

Assuming that $\mathrm{ARM_{int}} \approx \mathrm{ARM_{max}}$, (10) becomes

$$h_A \approx 100\, b\Delta V. \quad (11)$$

The experiments of *Kodama and Sun* [1990] imply that an h_A of 30% correlates with a ΔV of about 0.5 in clay with synthetic 0.45 by 0.075 μm magnetite needles that are probably single-domain. This h_A is consistent with (11) using *Anson and Kodama*'s [1987] experimental estimate that $b=0.63\pm0.18$ for clay with 0.45 by 0.075μm magnetite needles.

In our specimens, average ΔV is 0.62 ± 0.10, which according to (10) with $b=0.63\pm0.18$ should give an average $\mathrm{ARM_{min}/ARM_{max}}$ of 0.62 ± 0.2. The average observed $\mathrm{ARM_{min}/ARM_{max}}$ is 0.87 ± 0.01 (standard error). Much of the discrepancy is probably caused by the assumption in (9), (10), and (11) that ARM will not be acquired perpendicular to the long axes of the magnetite grains. This assumption that $\mathrm{ARM_\perp/ARM_\parallel}=0$ is justified for single-domain grains but not for pseudo-single-domain grains which dominate in most of our specimens. The five specimens that we measured have an average $\mathrm{ARM_\perp/ARM_\parallel}$ of 0.37 ± 0.17.

To deal with non zero $\mathrm{ARM_\perp/ARM_\parallel}$, *Jackson et al.* [1991] show theoretically that (9) should be modified as follows (rewriting their equations and assuming $\mathrm{ARM_{int}} = \mathrm{ARM_{max}}$):

$$\frac{\tan I_N}{\tan I} = \frac{(\mathrm{ARM_{min}/ARM_{max}})(1 + \mathrm{ARM_\perp/ARM_\parallel})}{1 - (\mathrm{ARM_\perp/ARM_\parallel})(\mathrm{ARM_{min}/ARM_{max}})} - \frac{2\,(\mathrm{ARM_\perp/ARM_\parallel})}{1 - (\mathrm{ARM_\perp/ARM_\parallel})(\mathrm{ARM_{min}/ARM_{max}})}. \quad (12)$$

Equation (10) should then similarly be modified to

$$\frac{\mathrm{ARM_{min}}}{\mathrm{ARM_{max}}} = \frac{(1 - b\Delta V) + 2\,(\mathrm{ARM_\perp/ARM_\parallel})}{1 + (2 - b\Delta V)(\mathrm{ARM_\perp/ARM_\parallel})}. \quad (13)$$

Equation (13), with $\mathrm{ARM_\perp/ARM_\parallel}\approx0.37$, $\Delta V\approx0.62$, and $b\approx0.63$, predicts $\mathrm{ARM_{min}/ARM_{max}}\approx0.85$, in agreement with the average observed $\mathrm{ARM_{min}/ARM_{max}}$ of 0.87. Equation (13) with $b=0.63$ also gives a better estimate than (10) when applied individually to the five specimens for which $\mathrm{ARM_\perp/ARM_\parallel}$ has been measured (see Table 3). The one exception is specimen 316-23-3-107, whose $\mathrm{ARM_\perp/ARM_\parallel}$ has presumably been overestimated (perhaps because of incomplete alignment of magnetite grain long axes).

Can ARM Anisotropy Detect and Correct Inclination Shallowing?

Jackson et al. [1991] suggested that (9) or, more generally, (12) should allow ARM anisotropy to be used to detect and correct for inclination shallowing in detrital remanence (including pDRM).

Equation (12) p edicts a relation between $\tan I_N/\tan I$ and $\mathrm{ARM_{min}/ARM_{max}}$ that depends on the m^gnetic particle anisotropy parameter $\mathrm{ARM_\perp/ARM_\parallel}$ as shown in Figure 7 for our observed range of $\mathrm{ARM_{min}/ARM_{max}}$ values. For $\mathrm{ARM_\perp/ARM_\parallel}=0$ (that is, for elongated single-domain grains), (12) predicts a linear relation between $\tan I_N/\tan I$ and $\mathrm{ARM_{min}/ARM_{max}}$. Note that the predicted relation remains approximately linear, with the line continuing to pass through (1.0, 1.0) provided that $\mathrm{ARM_\perp/ARM_\parallel}$ remains small compared to 1.0.

Kodama and Sun [1992] measured how $\tan I_N/\tan I$ and $\mathrm{ARM_z/ARM_x}$ changed during laboratory compaction of two clay-rich marine sediments containing magnetite of probable pseudo-single-domain grain size. Their results, shown by open and solid circles in Figure 7, are in reasonable agreement with (12), assuming $\mathrm{ARM_\perp/ARM_\parallel}$ of ~0.25 and ~0.55, respectively. Their results also fit reasonably well to straight lines passing close to (1.0, 1.0), as expected.

Equation (12) and these experiments of *Kodama and Sun* [1992] lead us to expect a linear correlation between $\tan I_N/\tan I$ and $\mathrm{ARM_{min}/ARM_{max}}$ in our limestones. This correlation, shown in Figure 8, is significant with 99% confidence (R=0.510, N=32). The equation of the least squares fit correlation line is

$$\frac{\tan I_N}{\tan I} = 2.32\,\left(\frac{\mathrm{ARM_{min}}}{\mathrm{ARM_{max}}}\right) - 1.48. \quad (14)$$

Its 2.32 ± 0.72 slope agrees with the ~2.4 slope of the approximately linear relation predicted by (12) using $\mathrm{ARM_\perp/ARM_\parallel}=0.37$ (the average of our five determinations in Table 3). Equation (14) with $\mathrm{ARM_{min}/ARM_{max}}=1$ predicts $\tan I_N/\tan I=0.84\pm0.25$, which does not differ significantly from 1.0. The ±0.25 standard deviation of $\tan I_N/\tan I$ values about the correlation line is probably due mainly to the effect of paleosecular variation on I_N.

These above results suggest the following method for detecting compaction-induced inclination shallowing in a suite of sediments deposited together in a field of unknown inclination I. Compaction-induced inclination shallowing is likely present if the ARM anisotropy is foliated in the bedding plane and there is significant correlation between $\tan I_N$ and $\mathrm{ARM_{min}/ARM_{max}}$. The correlation line's prediction of I_N when $\mathrm{ARM_{min}/ARM_{max}}=1$ will then be an estimate of I. This may underestimate I owing to the nonlinearity of (12) unless $\mathrm{ARM_\perp/ARM_\parallel}$ is small compared to 1.0 and $\mathrm{ARM_{min}/ARM_{max}}$ does not greatly differ from 1.0. (There may also be difficulties with nonlinearity in the early stages of compaction, judging by the experiments of *Kodama and Sun* [1992] on synthetic acicular single-domain magnetite in clay.) Another difficulty, if $\mathrm{ARM_\perp/ARM_\parallel}$ approaches 1.0, is that equidimensional magnetic grains will dominate. If compaction rotates these grains preferentially about horizontal axes, they can cause inclination shallowing (according to the theory of *Arason and Levi* [1990a]) but there will be no ARM anisotropy to warn of its presence. A rough prediction of average $\mathrm{ARM_\perp/ARM_\parallel}$ can be obtained by comparing the slopes of the theoretical lines of Figure 7 with the slope of the correlation line divided by the tangent of the estimate of I.

We now apply this method to data on Quarternary deep-sea clays that show inclination shallowing (published by *Collombat et al.* [1990] in a graph reproduced in larger format by *Jackson* [1991]). *Collombat et al.* [1990] found

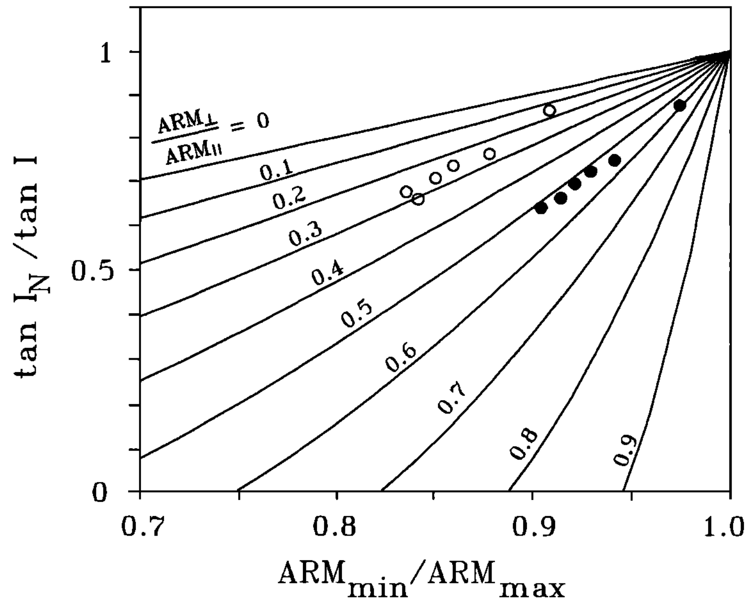

Fig. 7. The relation between tan I_N/ tan I and ARM_{min}/ARM_{max} predicted by (12) from *Jackson et al.* [1991] for various values of $ARM_{\parallel}/ARM_{\perp}$. The open and solid circles indicate observations by *Kodama and Sun* [1992] on the two clay-rich marine sediments that they progressively compacted in the laboratory.

a correlation between I-I_N and ARM_{min}/ARM_{max} and proposed to use (9) with ARM_{min}/ARM_{max} replaced by $(ARM_{min}/ARM_{max})^3$ to correct for inclination error. We do not recommend using this correction, because although it has some empirical basis, it lacks theoretical justification.

The data of *Collombat et al.* [1990] do show a correlation between tan I_N and ARM_{min}/ARM_{max} (Figure 9) that is significant with 99% confidence (R=0.614, N=22). This supports the presence of inclination error. (We assume that the ARM anisotropy is foliated in the bedding plane, as is generally true of the susceptibility anisotropy in this part of the core [*Shor et al.*, 1984].) The equation of the correlation line is

$$\tan I_N = 2.99 \left(\frac{ARM_{min}}{ARM_{max}}\right) - 1.41 . \qquad (15)$$

For $ARM_{min}/ARM_{max}=1$, the correlation line predicts I_N = 58° with a ±6° error estimated from the standard deviation of tan I_N values about the correlation line. (The slope of the correlation line divided by tan 58° compared with the slopes of the theoretical lines of Figure 7 predicts that average $ARM_{\perp}/ARM_{\parallel} \approx 0.25$. This is small compared to 1.0, suggesting that 58°±6° is a reliable estimate of I.) This 58°±6° estimate of field inclination does indeed agree with the 61° expected for these sediments.

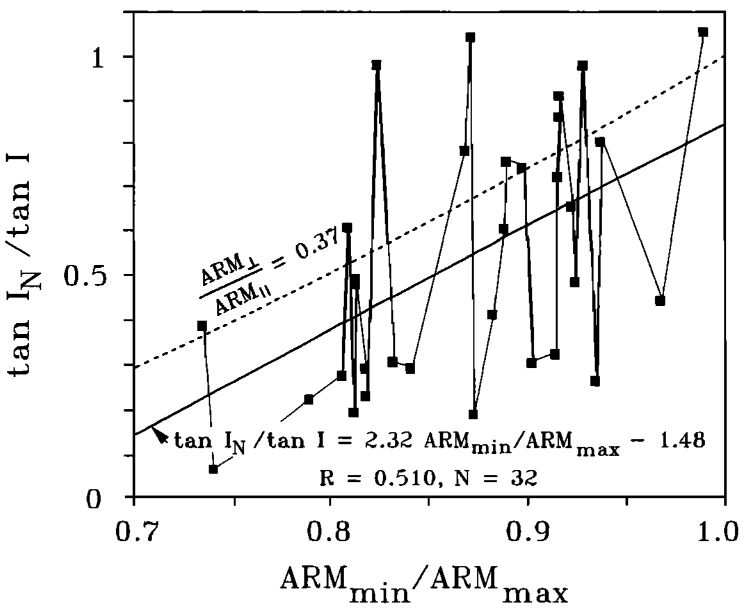

Fig. 8. The correlation observed between tan I_N/ tan I and ARM_{min}/ARM_{max} for our limestone specimens. The dashed line indicates the relation predicted by (12) using our average observed $ARM_{\perp}/ARM_{\parallel}$ of 0.37.

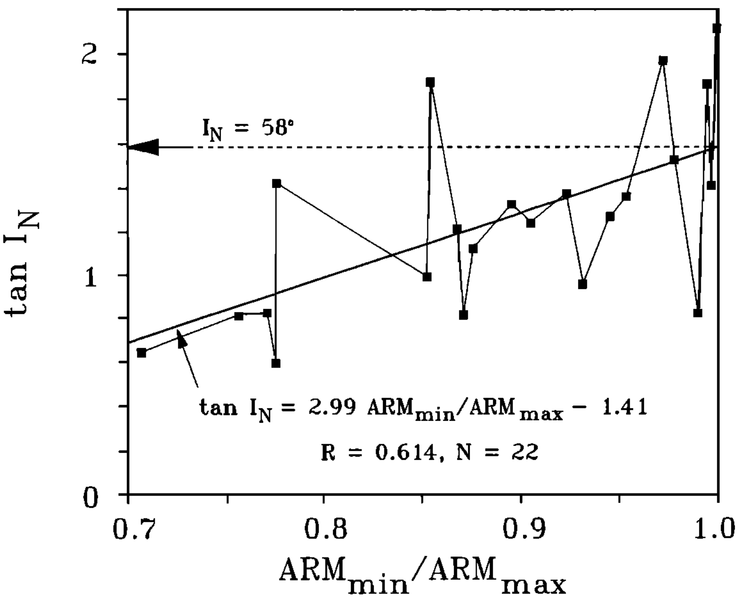

Fig. 9. The correlation observed between tan I_N and ARM_{min}/ARM_{max} using the data of *Collombat et al.* [1990] for the Quaternary deep-sea clays from 5 to 10 m depth in piston core RC22-14 [*Shor et al.*, 1984]. The correlation line predicts that $I_N = 58° \pm 6°$ when $ARM_{min}/ARM_{max} = 1$, in agreement with the 61° inclination expected of the Earth's field.

CONCLUSIONS

The following can be concluded about 34 Cretaceous deep-sea limestones that we studied from five Pacific plate DSDP sites reported to show inclination shallowing. (We omit specimen 288A-23-2-115 from these conclusions because its anisotropy was strongly foliated at a large angle to the bedding plane.)

1. Natural remanence above 20 mT coercivity retained approximately constant direction upon AF demagnetization, with inclination an average of 17° shallower than the average inclination of 44° expected from the APWP.

2. Natural remanence is likely carried by magnetite, mainly of pseudo-single-domain grain size (judging from coercivity, ratio of ARM to susceptibility, and comparison of ARM anisotropy with susceptibility anisotropy).

3. Natural remanence is likely a pDRM (judging from the fine grain size of the magnetite and from evidence of bioturbation).

4. The average inclination shallowing of 17° was likely induced by the average fractional compaction of 0.6 (estimated from porosity), which is consistent with compaction experiments [*Anson and Kodama*, 1987] and with theory [*Arason and Levi*, 1990*a*].

5. ARM_{min} is perpendicular to the bedding plane, with $ARM_{max} \approx ARM_{int}$, suggesting a compaction-induced ARM anisotropy. (Any anisotropy acquired upon deposition should have been destroyed by bioturbation.)

6. The average ARM_{min}/ARM_{max} of 0.87 was likely induced by the average fractional compaction of 0.6, which is consistent with theory (results by *Arason and Levi*, [1991*a*] and *Jackson et al.* [1991] combined) if the ability of the grains to acquire ARM perpendicular to their long axes is taken into account by using $ARM_{\perp}/ARM_{\parallel} \approx 0.37$ (the average of our five determinations).

7. A significant correlation between tan I_N/ tan I and ARM_{min}/ARM_{max} is observed in our limestones, as expected from theory [*Jackson et al.*, 1991] and from compaction experiments [*Kodama and Sun*, 1992]. The correlation line's slope of 2.3 ± 0.7 agrees with the slope of ~2.4 expected from theory using $ARM_{\perp}/ARM_{\parallel} \approx 0.37$.

8. Our limestone results suggest that compaction-induced inclination shallowing can be detected in a suite of fine-grained magnetite-bearing sedimentary rocks deposited at the same paleolatitude. Having shown that ARM_{min} is perpendicular to bedding and that $ARM_{max} \approx ARM_{int}$, look for a correlation between tan I_N and ARM_{min}/ARM_{max}. This correlation's prediction of I_N when $ARM_{min}/ARM_{max} = 1$ should estimate I corrected for inclination shallowing (assuming that $ARM_{\perp}/ARM_{\parallel}$ is small compared to 1.0). This method is shown to succeed for the data of *Collombat et al.* [1990] for Quaternary deep-sea clays.

Acknowledgments. This research was supported by a grant to J. Hodych from the Natural Sciences and Engineering Research Council of Canada and by a scholarship to S. Bijaksana from the Ministry of Education and Culture of the Republic of Indonesia. We thank G. Bode and S. Prinz of the ODP Repository in La Jolla, California, for assistance during sampling. We thank A. Aksu and R. Mason of our department for help with X ray diffraction and C. Hale of the University of Toronto for use of his susceptibility anisotropy meter. C. Langereis, B. Ellwood, and M. Jackson are thanked for useful comments on the text.

REFERENCES

Anson, G. L., and K. P. Kodama, Compaction-induced inclination shallowing of the post depositional remanent magnetization in a synthetic sediment, *Geophys. J. R. Astron. Soc.*, *88*, 673-692, 1987.

Arason, P., and S. Levi, Models of inclination shallowing during sediment compaction, *J. Geophys. Res.*, *95*, 4,481-4,499, 1990*a*.

Arason, P., and S. Levi, Compaction and inclination shallowing in deep-sea sediments from the Pacific Ocean, *J. Geophys. Res.*, *95*, 4,501-4,510, 1990*b*.

Bijaksana, S., Magnetic anisotropy of Cretaceous deep sea sedimentary rocks from the Pacific plate, M.Sc. thesis, 162 pp., Mem. Univ. of Newfoundland, St. John's, Canada, 1991.

Bijaksana, S., and J. P. Hodych, Magnetic anisotropy evidence of compaction-induced inclination shallowing in Cretaceous deep-sea sedimentary rocks from the Pacific plate (abstract), *Eos Trans. AGU, 73,* (14) Spring Meeting Suppl., 100-101, 1992.

Blow, R. A., and N. Hamilton, Effect of compaction on the acquisition of a detrital remanent magnetization in fine-grained sediments, *Geophys. J. R. Astron. Soc., 52,* 13-23, 1978.

Butler, R. F., *Paleomagnetism*, 319 pp., Blackwell, Oxford, 1992.

Celaya, M. A., and B. M. Clement, Inclination shallowing in deep-sea sediments from the North Atlantic, *Geophys. Res. Lett., 15,* 52-55, 1988.

Collombat, H., P. Rochette, and M. J. Jackson, Possible correction of the inclination error in deep sea sediments using the anisotropy of anhysteretic remanence (abstract), *Eos Trans. AGU, 71,* 1288, 1990.

Deamer, G. A., and K. P. Kodama, Compaction-induced inclination shallowing in synthetic and natural clay-rich sediments, *J. Geophys. Res., 95,* 4,511-4,529, 1990.

deMenocal, P. B., W. F. Ruddiman, and D. V. Kent, Depth of post-depositional remanence acquisition in deep-sea sediments: A case study of the Brunhes-Matuyama reversal and oxygen isotopic stage 19.1, *Earth Planet. Sci. Lett., 99,* 1-13, 1990.

Dunlop, D. J., The rock magnetism of fine particles, *Phys. Earth Planet. Inter., 26,* 1-26, 1981.

Ellwood, B. B., Bioturbation: Minimal effects on the magnetic fabric of some natural and experimental sediments, *Earth Planet. Sci. Lett., 67,* 367-376, 1984.

Ellwood, B. B., F. Hrouda, and J. J. Wagner, Symposia on magnetic fabrics: Introductory comments, *Phys. Earth Planet. Inter., 51,* 249-252, 1988.

Freeman, R., Magnetic mineralogy of pelagic limestones. *Geophys. J. R. Astron. Soc., 85,* 433-452, 1986.

Girdler, R. W., The measurement and computation of anisotropy of magnetic susceptibility of rocks, *Geophys. J. R. Astron. Soc., 5,* 34-44, 1961.

Gordon, R. G., Late Cretaceous apparent polar wander of the Pacific plate: Evidence for a rapid shift of the Pacific hotspots with respects to the spin axis, *Geophys. Res. Lett., 10,* 709-712, 1983.

Gordon, R. G., Test for bias in paleomagnetically determined palaeolatitudes from Pacific plate Deep Sea Drilling Project sediments, *J. Geophys. Res., 95,* 8,397-8,404, 1990.

Hamilton, E. L., Variations of density and porosity with depth in deep-sea sediments, *J. Sediment. Petrol., 46,* 280-300, 1976.

Harland, W. B., et al., *A Geologic Time Scale 1989*, 263 pp., Cambridge University Press, New York, 1990.

Hodych, J. P., Magnetic hysteresis as a function of low temperature in rocks: Evidence for internal stress control of remanence in multi-domain and pseudo-single-domain magnetite, *Phys. Earth Planet. Inter., 64,* 21-36, 1990.

Howell, L. G., J. D. Martinez, and E. H. Statham, Some observations on rock magnetism, *Geophysics, 23,* 285-298, 1958.

Irving, E., and G. Pullaiah, Reversals of the geomagnetic field, magnetostratigraphy and relative magnitude of paleosecular variation in the Phanerozoic, *Earth Sci. Rev., 12,* 35-64, 1976.

Jackson, M., Anisotropy of magnetic remanence: A brief review of mineralogical sources, physical origins and geological applications, and comparison with susceptibility anisotropy, *Pure Appl. Geophys., 136,* 1-28, 1991.

Jackson, M. J., S. K. Banerjee, J. A. Marvin, R. Lu, and W. Gruber, Detrital remanence, inclination errors and anhysteretic remanence anisotropy: Quantitative model and experimental results, *Geophys. J. Int., 104,* 95-103, 1991.

King, J. W., S. K. Banerjee, and J. Marvin, A new rock-magnetic approach to selecting sediments for geomagnetic paleointensity studies: Application to paleointensity for the last 4000 years, *J. Geophys. Res., 88,* 5,911-5,921, 1983.

Kirschvink, J. L., The least squares line and plane and the analysis of paleomagnetic data, *Geophys. J. R. Astron. Soc., 62,* 699-718, 1980.

Kodama, K. P., and W. W. Sun, SEM and magnetic fabric study of a compacting sediment, *Geophys. Res. Lett., 17,* 795-798, 1990.

Kodama, K. P., and W. W. Sun, Magnetic anisotropy as a correction for compaction-caused paleomagnetic inclination shallowing, *Geophys. J. Int., 111,* 465-469, 1992.

McCabe, C., M. Jackson, and B. B. Ellwood, Magnetic anisotropy in the Trenton Limestone: Results of a new technique, anisotropy of anhysteretic susceptibility, *Geophys. Res. Lett., 12,* 333-336, 1985.

McFadden, P. L., and A. B. Reid, Analysis of palaeomagnetic inclination data, *Geophys. J. R. Astron. Soc., 69,* 307-319, 1982.

Potter, D. K., and A. Stephenson, Field-impressed anisotropies of magnetic susceptibility and remanence in minerals, *J. Geophys. Res., 95,* 15,573-15,588, 1990.

Reijers, T. J. A., and K. J. Hsü, *Manual of Carbonate Sedimentology: A Lexicographical Approach*, 302 pp., Academic, San Diego, Calif., 1986.

Rochette, P., Inverse magnetic fabric in carbonate-bearing rocks, *Earth Planet. Sci. Lett., 90,* 229-237, 1988.

Rochette, P., M. Jackson, and C. Aubourg, Rock magnetism and the interpretation of anisotropy of magnetic susceptibility, *Rev. Geophys., 30,* 209-226, 1992.

Sager, W. W., and M. S. Pringle, Mid-Cretaceous to early Tertiary apparent polar wander path of the Pacific plate, *J. Geophys. Res., 93,* 11,753-11,771, 1988.

Shive, P. N., Suggestions for the use of SI units in magnetism, *Eos Trans. AGU, 67,* 25, 1986.

Shor, A.N., D.V. Kent, and R.D. Flood, Contourite or turbidite?: magnetic fabric of fine-grained Quaternary sediments, Nova Scotia continental rise, in *Fine Grained Sediments: Deep-Water Processes and Facies*, edited by D. A. V. Stow and D. J. W. Piper, pp. 257-273, Blackwell, Oxford, 1984.

Steiner, M. B., Paleomagnetism of the Cretaceous section, site 462, in *Initial Reports of the Deep Sea Drilling Project, vol. LXI*, pp. 711-716, U.S. Government Printing Office, Washington, D.C., 1981.

Stephenson, A., and D. K. Potter, Some aspects of the measurement of magnetic anisotropy, in *Geomagnetism and Paleomagnetism*, edited by S. K. Runcorn, D. C. Tozer, and A. Soward, pp. 271-278, Kluwer Academic, Norwell, Mass., 1989.

Stephenson, A., S. Sadikun, and D. K. Potter, A theoretical and experimental comparison of the anisotropies of magnetic susceptibility and remanence in rocks and minerals, *Geophys. J. R. Astron. Soc., 84,* 185-200, 1986.

Stow, D. A. V., and D. J. W. Piper, Deep-water fine-grained sediments; history, methodology and terminology, in *Fine Grained Sediments: Deep-Water Processes and Facies*, edited by D. A. V. Stow, and D. J. W. Piper, pp. 3-14, Blackwell, Oxford, 1984.

Tarduno, J.A., Absolute inclination value from deep sea sediments: A reexamination of the Cretaceous Pacific record, *Geophys. Res. Lett., 17,* 101-104, 1990.

Tauxe, L., and G. Wu, Normalized remanence in sediments of the western equatorial Pacific: Relative paleointensity of the geomagnetic field?, *J. Geophys. Res., 95,* 12,337-12,350, 1990.

Verosub, K. L., Depositional and postdepositional processes in the magnetization of sediments, *Rev. Geophys. Space Phys., 15,* 129-143, 1977.

Zonenshain, L. P., M. V. Kononov, and L. A. Savostin, Pacific and Kula/Eurasia relative motions during the last 130 Ma and their bearing on orogenesis in Northeast Asia, in *Circum-Pacific Orogenic Belts and Evolution of the Pacific Ocean Basin, Geodyn. Ser.* vol. 18, edited by J. W. H. Monger, and J. Francheteau, pp. 29-47, AGU, Washington, D.C., 1987.

S. Bijaksana and J. P. Hodych, Department of Earth Sciences, Memorial University of Newfoundland, St. John's, Newfoundland, A1B 3X5 Canada.

(Received January 20, 1993;
revised July 6, 1993;
accepted July 20, 1993.)